Available online at www.sciencedirect.com

ScienceDirect

IFAC Papers Online CONFERENCE PAPER ARCHIVE

IFAC PapersOnLine 52-15 (2019) 495–500

Constrained port Hamiltonian formulation of multiscale distributed parameter IPMC systems ⋆

Ning Liu, * **Yongxin Wu,** * **Yann Le Gorrec** *

* *FEMTO-ST CNRS UMR 6174, Université Bourgogne Franche-Comté, 26 chemin de l'épitaphe, F-25030 Besançon, France. (e-mail: ning.liu@femto-st.fr; yongxin.wu@femto-st.fr; yann.le.gorrec@ens2m.fr).*

Abstract: In this paper, a constrained distributed parameter port-Hamiltonian model of the ionic polymer metal composite actuator is proposed. This model describes the multiscale structure of the system. Submodels are coupled by boundary multi-scale elements. In order to preserve the causality of the system, Lagrangian multipliers are introduced to deal with the coupling between the electro-stress diffusion in the polymer and the flexible beam structure of the actuator. Finally, a structure-preserving discretization scheme and some appropriate projections are used to derive an explicit model suitable for simulation. The accuracy of the model is verified using experimental data.

Keywords: Constrained port Hamiltonian system, infinite dimensional system, multi-scale modeling, model reduction, IPMC actuator

1. INTRODUCTION

Ionic polymer metal composites (IPMCs) are electro-active systems that can be used either as an actuator or a sensor. Among the diversity of electro-active materials such as piezoelectric materials, magnetostrictive materials etc., IPMCs are more and more used in different application fields, e.g biomedical applications, bio-manipulation and micro- or macro-electromechanical systems (Shahinpoor, 2016) due to their low-cost voltage, large deformation, wide working frequency ranges and their capability of working in aqueous environments. IPMCs consist of a double electrode layer filled with a polyelectrolyte gel. Cations and solvent molecules migrate toward the cathode when a difference in the electric potential is imposed across the two terminals of its double electrode layer. As a consequence, the cathode side swells while the anode side shrinks, entailing a bending effect to the anode side (Park et al., 2010). Based on its physical structure and working principle, various models for IPMCs have been proposed in the literature, going from the black box model (Xiao and Bhattacharya, 2001) to models using more physical insight (Shahinpoor, 2016; Branco et al., 2012).

A powerful tool for the modeling and control of complex multi-physical nonlinear systems, called port-Hamiltonian approach, has been introduced and developed in the last decade (Maschke and van der Schaft, 1992).

The first port-Hamiltonian modeling of IPMC actuators has been proposed in (Nishida et al., 2011). This model consists in three sub-components which are multi-scale, and are all described by distributed parameter systems interconnected each other using boundary multi-scale (BMS) coupling elements. By considering the out-domain variables as uniform (Nishida et al., 2011), the BMS works as a differential gyrator, which lets the out-domain variables be multiplied by a characteristic function, meanwhile, makes the in-domain variables be integrated spatially. However, there exists a conflict of causality due to the coupling of the mechanical properties of the gel and the mechanical structure (passive moment coupling of equation (54) in (Nishida et al., 2011)). To deal with this conflict, we consider a multiscale model including Lagrange multiplier to account for these mechanical constraints, and numerically simulate the model more precisely, which includes all coupling relations. The resulting system of differential algebraic equation (DAE) is reduced to an ordinary differential equation (ODE) using coordinates projection.

The present paper is organized as follows. In Section 2 is given the constrained port Hamiltonian model of the multiscale IPMC. In Section 3, a finite difference method on staggered grids is applied to discretize the system and the final model is reduced by using coordinates projection. Numerical simulation and conclusions are given in Section 4 and 5, respectively.

2. MODELING OF IPMC

The IPMC under investigation (cf. Fig. 1) is of length L, width b and thickness h. It consists of three sub-systems at different scales as shown in Fig. 1.

First, an electrical model, which is at a scale of nanometer, is used to represent the fractal-like structure of the double electrical layers. The dynamics of the polyelectolyte gel, at a scale of 100 μm, is described by an electro-stress diffusion coupling model. At last, the global mechanical

⋆ This work is supported by the INFIDHEM project and the Bourgogne-Franche-comté Region ANER project under the reference code ANR-16-CE92-0028 and 2018Y-06145, respectively.

10.1016/j.ifacol.2019.11.724

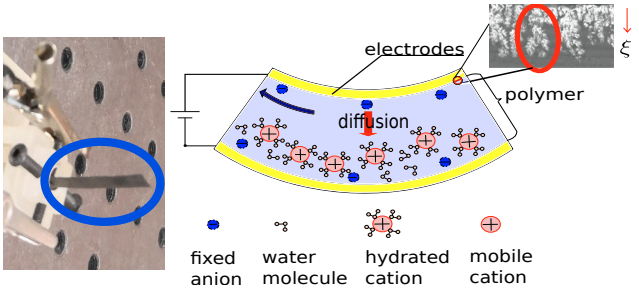

Fig. 1. IPMC structure and shape (Shahinpoor, 2016).

deformation of IPMC is described by the Timoshenko beam model, whose scale is centimeter. Both the electrical system and the electro-stress diffusion system are modeled locally, whereas the mechanical beam system is modeled globally. In this section, we present each sub-system and their coupling through boundary or in domain multiscale elements.

2.1 Electrical system

The two electrodes of Fig. 1 are modeled by the distributed RC circuit. The voltage V is supposed to be uniformly distributed on the double layers electrodes.

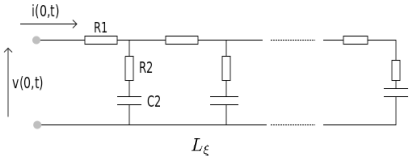

Fig. 2. Infinite dimension electrical system.

With the idea of (Nishida et al., 2008), (Nishida et al., 2011), each fractal-like structure (see the red circle in Fig. 1) is referenced as ξ in a virtual coordinate. L_ξ denotes the length of each fractal-like structure, R_1 is the resistance between two adjacent branches of fractal-like structure, and R_2 and C_2 are the resistive and capacitive impedance of each branch, respectively (Bao et al., 2002). Each fractal-like structure is connected to the electro-active gel through its boundary at $\xi = 0$.
The continuity equation and the Kirchhoff's current law (KCL) yield:

$$\frac{\partial Q(\xi,t)}{\partial t} = -\frac{\partial i(\xi,t)}{\partial \xi}, \tag{1}$$

where $Q(\xi,t)$ is the charge density of each capacitor.
By applying the Kirchoff's voltage law (KVL), one gets :

$$\frac{\partial v(\xi,t)}{\partial \xi} + R_1(\xi) i(\xi,t) = 0. \tag{2}$$

Let $v(0,t) = V + V_c$, and $i(0,t) = I$, where V_c corresponds to the voltage coming from the gel. By defining (Nishida et al., 2008):

$$\begin{aligned}
e_1(\xi,t) &= v(\xi,t) = \frac{Q(\xi,t)}{C_2(\xi,t)} + R_2(\xi)\frac{\partial Q(\xi,t)}{\partial t},\\
f_{r1}(\xi,t) &= \partial/\partial\xi \left(v_{c2}(\xi,t) + R_2(\xi)\partial Q(\xi,t)/\partial t\right),\\
f_1(\xi,t) &= -\frac{\partial Q(\xi,t)}{\partial t},\\
e_{r1}(\xi,t) &= -f_{r1}(\xi,t)/R_1(\xi),
\end{aligned}$$

and combining equation (2), equation (1) can be written on the form [1]

$$\begin{aligned}
&\begin{pmatrix} f_1 \\ f_{r1} \end{pmatrix} = \begin{pmatrix} 0 & \partial_\xi \\ \partial_\xi & 0 \end{pmatrix} \begin{pmatrix} e_1 \\ e_{r1} \end{pmatrix},\\
&\begin{pmatrix} f_{\partial\xi} \\ e_{\partial\xi} \end{pmatrix} = \begin{pmatrix} (e_1(0)\ e_1(L_\xi))^T \\ (-e_{r1}(0)\ e_{r1}(L_\xi))^T \end{pmatrix} = \begin{pmatrix} (V+V_c\ e_1(L_\xi))^T \\ (-I\ e_{r1}(L_\xi))^T \end{pmatrix}.
\end{aligned} \tag{3}$$

Assuming that the impedances are infinite, the current at the endpoint of each fractal structure is zero, namely $i(L_\xi,t) = e_{r1}(L_\xi) = 0$ (Nishida et al., 2011).

2.2 Electro-stress diffusion system

An electro-stress diffusion coupling model is considered to describe the swelling and shrinking dynamics in the gel (Nishida et al., 2011). Compared to the diffusion in the liquid phase of the gel, the deformation of the solid phase is so fast that it is considered as quasi-static. Consequently, the mechanical dynamics of the gel is not represented explicitly, and the radius of curvature of the gel is derived from the rotational angle of the beam, leading to an algebraic constraint.

Deformation of the solid phase This deformation is assumed to be symmetric. The schematic is shown in Fig. 3. The radius of curvature $R(x,t)$ fluctuates along the x-axis,

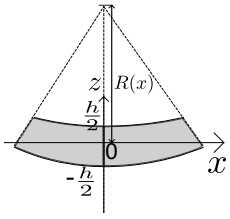

Fig. 3. Deformation of gel in one dimension.

but is assumed to be locally homogeneous (Nishida et al., 2008), i.e. $\partial R(x,t)/\partial x = 0$ always holds in each z domain. The displacement of each volume point projected in Cartesian coordinate is given by:

$$u_z = u_z(z,t),\ u_x = \frac{z}{R(x,t)}x,\ u_y = \frac{z}{R(x,t)}y. \tag{4}$$

The swelling ratio $f_{s1}(z,x,t)$ of the solid part is defined as the divergence of the displacement tensor:

$$\begin{aligned}
f_{s1}(z,x,t) = \nabla \cdot u &= \begin{bmatrix} \frac{\partial}{\partial x} & \frac{\partial}{\partial y} & \frac{\partial}{\partial z} \end{bmatrix} \begin{bmatrix} u_x & u_y & u_z \end{bmatrix}^T\\
&= \frac{2z}{R(x,t)} + \frac{\partial u_z}{\partial z}.
\end{aligned} \tag{5}$$

According to the hypothesis of symmetric deformation, the linear formulation about the stress tensor and the displacement is expressed as:

$$\sigma_{ij} = K\sum_k \frac{\partial u_k}{\partial x_k}\delta_{ij} + G\left(\frac{\partial u_i}{\partial x_j} + \frac{\partial u_j}{\partial x_i} - \frac{2}{3}\sum_k \frac{\partial u_k}{\partial x_k}\delta_{ij}\right), \tag{6}$$

where K and G are the bulk modulus and the shear modulus of the gel, respectively, and δ_{ij} is the Dirichlet function. The stresses are average variables in the IPMC. Further informations on different stresses of IPMC model

[1] For the purpose of simplicity, $\partial/\partial\xi$ is denoted as ∂_ξ and the symbol t is omitted in the following context.

are available in (Zhu et al., 2012).
As a result, equation (4) and (6) yield the following expression:

$$\begin{aligned}\sigma_{xx}(z,x,t) &= \left(K-\frac{2}{3}G\right)f_{s1}(z,x,t)+\frac{2G}{R(x,t)}z,\\ \sigma_{zz}(z,x,t) &= \left(K+\frac{4}{3}G\right)f_{s1}(z,x,t)-\frac{4G}{R(x,t)}z.\end{aligned} \tag{7}$$

Dynamics of the liquid phase Two coupled phenomena can be distinguished in the liquid phase: electro-osmosis, and water transport. These coupled phenomena were formulated in the work of (De Gennes et al., 2000), covering the transport of ions and the solvent:

$$\begin{aligned}\mathbf{j}_e &= -\sigma_e\nabla\psi-\lambda\nabla p,\\ \mathbf{j}_s &= -k\nabla p-\lambda\nabla\psi,\end{aligned} \tag{8}$$

where $\mathbf{j}_e$ and $\mathbf{j}_s$ represent the electric current density and the water flux density, respectively. σ_e is the conductance, λ stands for the Onsager's coupling constant, k denotes the Darcy's permeability, ψ is the electric field, and p represents the water pressure in the network (De Gennes et al., 2000).
It is supposed that the liquid goes only in the z direction, so $\nabla p = \partial p/\partial z$ is the mechanical force. The bulk region of the gel satisfies the charge neutrality condition, namely $\nabla\mathbf{j}_e = 0$. The incompressibility of poly-electrolyte gel is also assumed in this work (Yamaue et al., 2005), i.e.:

$$p=\sigma_{zz}=\left(K+\frac{4}{3}G\right)f_{s1}(z,x,t)-\frac{4G}{R(x,t)}z. \tag{9}$$

Thus, the gradient of pressure can be calculated as:

$$\nabla p=\frac{\partial p}{\partial z}=\left(K+\frac{4}{3}G\right)\frac{\partial f_{s1}(z,x,t)}{\partial z}-\frac{4G}{R(x,t)}. \tag{10}$$

So equation (8) can be rewritten as:

$$\begin{aligned}\mathbf{j}_s(z,x,t) &= \frac{\lambda}{\sigma_e}\mathbf{j}_e+\left(\frac{\lambda^2}{\sigma_e}-k\right)\nabla p\\ &= -D'\frac{\partial f_{s1}(z,x,t)}{\partial z}+\mathbf{1}_Z\frac{\lambda}{\sigma_e}\mathbf{j}_e(t)+\mathbf{1}_Z\Phi(x,t),\end{aligned} \tag{11}$$

with

$$D'=\left(k-\frac{\lambda^2}{\sigma_e}\right)\left(K+\frac{4}{3}G\right),\Phi(x,t)=\left(k-\frac{\lambda^2}{\sigma_e}\right)\frac{4G}{R(x,t)}, \tag{12}$$

where $\mathbf{1}_Z$ stands for the characteristics function of domain z. It distributes the boundary values $\lambda/\sigma_e\mathbf{j}_e(t)$ and $\Phi(x,t)$ as uniform constants into z domain.
In the liquid phase, a swelling ratio f_{s2} is also introduced. It follows the conservation law that:

$$\frac{\partial f_{s2}(z,x,t)}{\partial t}=-\frac{\partial\mathbf{j}_s(z,x,t)}{\partial z}. \tag{13}$$

This equation can then be reformulated in the PHS framework as:

$$\begin{pmatrix}f_2\\ f_{r2}\end{pmatrix}=\begin{pmatrix}-\frac{\partial f_{s2}}{\partial t}\\ \frac{\partial f_{s2}}{\partial z}\end{pmatrix}=\begin{pmatrix}0 & \partial_z\\ \partial_z & 0\end{pmatrix}\begin{pmatrix}f_{s2}\\ -D'\frac{\partial f_{s1}}{\partial z}\end{pmatrix}. \tag{14}$$

The effort and the boundary variables are:

$$\begin{pmatrix}e_2\\ e_{r2}\end{pmatrix}=\begin{pmatrix}f_{s2}\\ -D'\frac{\partial f_{s1}}{\partial z}\end{pmatrix},\ \begin{pmatrix}f_{\partial z}\\ e_{\partial z}\end{pmatrix}=\begin{pmatrix}-D'\frac{\partial f_{s1}}{\partial z}\left(-\frac{h}{2}\right)\\ -D'\frac{\partial f_{s1}}{\partial z}\left(\frac{h}{2}\right)\\ -f_{s2}\left(-\frac{h}{2}\right)\\ f_{s2}\left(\frac{h}{2}\right)\end{pmatrix}. \tag{15}$$

Since the solid and liquid phases are strongly mixed with each other, we have $f_{s1}=f_{s2}=f_s$.
As hinted by equation (15), $\mathbf{1}_Z\lambda/\sigma_e\mathbf{j}_e(t)$ and $\mathbf{1}_Z\Phi(x,t)$ do not appear explicitly in the dynamics, while they play a role of input in order to match the impermeable assumption $\mathbf{j}_s(\pm h/2,t)=0$.

Bending moments generated in the gel According to (Nishida et al., 2008), the stress σ_{xx} can be divided into two parts: the active one $\sigma_a=(K-2/3G)f_s(z,x,t)$ related to the active swelling of the gel, and its passive counterpart $\sigma_p=2G/R(x,t)z$ corresponding to the storing energy.
The active stress can generate an active moment M_a:

$$M_a(x,t)=\int_{-\frac{h}{2}}^{\frac{h}{2}}\sigma_a(z,x,t)bzdz=\int_{-\frac{h}{2}}^{\frac{h}{2}}B_af_s(z,x,t)dz, \tag{16}$$

with $B_a(z)=(K-2/3G)bz$.
Besides, the passive moment M_p comes from the passive stress σ_p:

$$M_p(x,t)=\int_{-\frac{h}{2}}^{\frac{h}{2}}\sigma_p(z,x,t)bzdz=\frac{Gbh^3}{6R(x,t)}. \tag{17}$$

Regarding to the mechanical model along x-axis, the curvature $1/R$ is related to the angular strain $\partial\theta/\partial x$ of the IPMC via the geometric relationship:

$$\frac{1}{R(x,t)}+\frac{\partial\theta}{\partial x}=0. \tag{18}$$

At the initial phase of actuation, the active moment M_a is much larger than the passive moment M_p, as evident from the phenomenon of quick bending of IPMC. As the curvature increases gradually, M_p is getting larger than M_a, which makes the IPMC to bend back slowly.

Coupling with the electrical system In light of equation (11), the interconnection between the electro-stress diffusion system and the electrical system is through boundary variables as $\mathbf{1}_Z\lambda/\sigma_e\mathbf{j}_e(t)$, $\partial f_s/\partial z$ and I, V_c. $\mathbf{j}_e$ can be related to I by:

$$\mathbf{j}_e(t)=\frac{1}{Lb}I(t). \tag{19}$$

Given that the two pairs of energy variables $\mathbf{1}_Z\lambda/\sigma_e\mathbf{j}_e(t)$, $\partial f_s/\partial z$ and I, V_c are of different scales and are defined in domains z and ξ respectively, a coupling element BMS is proposed to realize the interconnection (Nishida et al., 2011), as represented in Fig. 4.
By crossing the BMS, $\lambda/\sigma_e\mathbf{j}_e(t)$ is multiplied by the characteristic function $\mathbf{1}_Z$, which signifies an integration in domain z. $f_s|_{\partial z}$ denotes the space integration of $\partial f_s/\partial z$ with $f_s|_{\partial z}=f_s(h/2,t)-f_s(-h/2,t)$. Based on the power conservation law, $f_s|_{\partial z}$ is transformed into voltage $V_c(t)$ via the gyrator GY:

$$V_c(t)=-\frac{\lambda}{\sigma_e b}f_s(t)|_{\partial z}=-\frac{\lambda}{\sigma_e b}\left(f_s(\frac{h}{2},t)-f_s(-\frac{h}{2},t)\right). \tag{20}$$

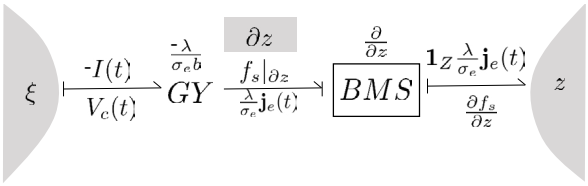

Fig. 4. Bond graph of the coupling between the domain z and ξ.

Coupling with the mechanical system At the macro-scale, the electro-stress diffusion model connects with the mechanical model through two bending moments, M_a and M_p, and the angular velocity $\partial\theta(x,t)/\partial t$.

2.2.5.1. Coupling through the active moment In view of the power conservation, an additional term is added into equation (13) to match the output of active moment:

$$\frac{\partial f_s(z,x,t)}{\partial t} = -\frac{\partial \mathbf{j}_s(z,t)}{\partial z} + \mathbf{1}_Z B_a \frac{\partial\theta(x,t)}{\partial t}. \tag{21}$$

The latter term can be regarded as a diffusion term of the mass conservation, since the gel consists of multiple molecules.
The bond graph of this interconnection is similar to the one in Fig. 4.

2.2.5.2. Coupling through the passive moment As for the coupling via the passive moment M_p, it is supposed to make the connection with $\Phi(t)$, since both the gel model and the beam model have the same curvature, $1/R(t)$ and $\partial\theta/\partial x$. Because Φ is a flow source for this electro-stress diffusion system and M_p is the output of this system, a Lagrangian multiplier $\lambda_{\mathbf{L}}$ is proposed here to deal with the causality, as shown in Fig. 5. where $A = B_p$ with

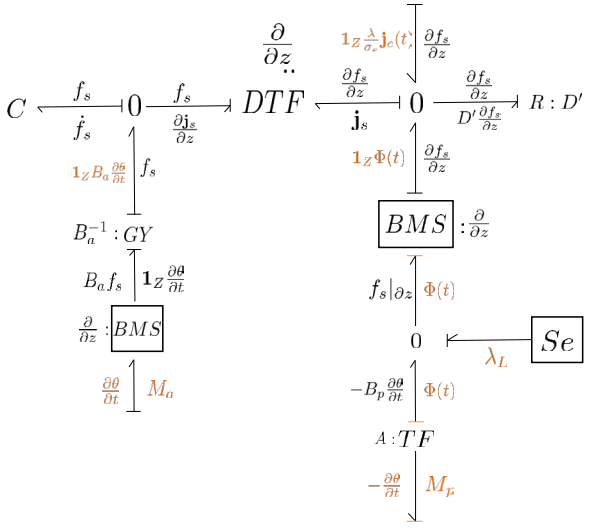

Fig. 5. Bond graph of the coupling through M_a, M_p and $\partial\theta/\partial t$.

$$B_p = \frac{bh^3}{24}\left(k - \frac{\lambda^2}{\sigma_e}\right)^{-1}.$$

The relations between Φ and M_p, and $f_s|_{\partial z}$ and $\partial\theta/\partial t$ are expressed as follows:

$$\begin{aligned} M_p(x,t) &= \Phi(x,t)B_p, \\ \frac{\partial\theta(x,t)}{\partial t} &= B_p^{-1}\left[f_s\left(\frac{h}{2},x,t\right) - f_s\left(-\frac{h}{2},x,t\right)\right]. \end{aligned} \tag{22}$$

With the Lagrangian $\lambda_{\mathbf{L}} = \Phi$, equation (22) is rewritten as:

$$\begin{aligned} \begin{pmatrix} 1 \\ B_p \end{pmatrix}\lambda_{\mathbf{L}} &= \begin{pmatrix} \lambda_{\mathbf{L}} \\ B_p\lambda_{\mathbf{L}} \end{pmatrix} = \begin{pmatrix} \Phi \\ M_p \end{pmatrix}, \\ (1\ B_p)\begin{pmatrix} f_s|_{\partial z} \\ \frac{-\partial\theta}{\partial t} \end{pmatrix} &= f_s|_{\partial z} - B_p\frac{\partial\theta}{\partial t} = 0, \end{aligned} \tag{23}$$

which reveals that the arrow of the Lagrangian multiplier in the bond graph Fig. 5 is an effort source with zero flow. This ensures the power conservation. Accordingly, equation (15) changes to:

$$\begin{aligned} \begin{pmatrix} f_2 \\ f_{r2} \end{pmatrix} &= \begin{pmatrix} 0 & \partial_z \\ \partial_z & 0 \end{pmatrix}\begin{pmatrix} e_2 \\ e_{r2} \end{pmatrix} + \begin{pmatrix} -B_a\frac{\partial\theta(x,t)}{\partial t} \\ 0 \end{pmatrix}, \\ \begin{pmatrix} f_{\partial z} \\ e_{\partial z} \end{pmatrix} &= \begin{pmatrix} \left(-D'\frac{\partial f_s}{\partial z}\left(-\frac{h}{2}\right)\ -D'\frac{\partial f_s}{\partial z}\left(\frac{h}{2}\right)\right)^T \\ \left(-f_s\left(-\frac{h}{2}\right)\ f_s\left(\frac{h}{2}\right)\right)^T \end{pmatrix}. \end{aligned} \tag{24}$$

2.3 Mechanical system

The mechanical deformation of IPMC can be represented by a classic Timoshenko beam with $x \in [0, L]$. The dynamics equation is reformulated under port Hamiltonian framework as (Villegas, 2007):

$$\frac{\partial}{\partial t}\begin{pmatrix} x_3(x,t) \\ x_4(x,t) \\ x_5(x,t) \\ x_6(x,t) \end{pmatrix} = \begin{pmatrix} 0 & \partial_x & 0 & -1 \\ \partial_x & 0 & 0 & 0 \\ 0 & 0 & 0 & \partial_x \\ 1 & 0 & \partial_x & 0 \end{pmatrix}\begin{pmatrix} e_3(x,t) \\ e_4(x,t) \\ e_5(x,t) \\ e_6(x,t) \end{pmatrix} + \begin{pmatrix} 0 \\ 0 \\ 0 \\ 1 \end{pmatrix} M_{ext}, \tag{25}$$

where $x_3(x,t) = \partial_x\omega(x,t) - \theta(x,t)$, $x_4(x,t) = \rho A(x)\partial_t\omega(x,t)$, $x_5(x,t) = \partial_x\theta(x,t)$, $x_6(x,t) = \rho I(x)\partial_t\theta(x,t)$, $e_3 = GA(x)x_3(x,t)$, $e_4 = \frac{1}{\rho A(x)}x_4(x,t)$, $e_5 = EI(x)x_5(x,t)$, $e_6 = \frac{1}{\rho I(x)}x_6(x,t)$.
The distributed bending moment comes from the electro-stress diffusion system, and reads:

$$M_{ext} = M_a + M_p. \tag{26}$$

According to (Le Gorrec et al., 2005), the boundary variables are calculated as:

$$\begin{pmatrix} f_{\partial x} \\ e_{\partial x} \end{pmatrix} = \begin{pmatrix} (e_4(0)\ e_3(L)\ e_6(0)\ e_5(L))^T \\ (-e_3(0)\ e_4(L)\ -e_5(0)\ e_6(L))^T \end{pmatrix}. \tag{27}$$

2.4 Global system

The above three subsystems can be connected to a global system, which is expressed as:

$$\underbrace{\begin{pmatrix} f_1 \\ f_{r1} \\ f_2 \\ f_{r2} \\ f_3 \\ f_4 \\ f_5 \\ f_6 \end{pmatrix}}_{f} = \underbrace{\begin{pmatrix} 0 & \partial_\xi & 0 & 0 & 0 & 0 & 0 & 0 \\ \partial_\xi & 0 & 0 & 0 & 0 & 0 & 0 & 0 \\ 0 & 0 & 0 & \partial_z & 0 & 0 & 0 & -\mathbf{1}_Z B_a \\ 0 & 0 & \partial_z & 0 & 0 & 0 & 0 & 0 \\ 0 & 0 & 0 & 0 & 0 & \partial_x & 0 & -1 \\ 0 & 0 & 0 & 0 & \partial_x & 0 & 0 & 0 \\ 0 & 0 & 0 & 0 & 0 & 0 & 0 & \partial_x \\ 0 & 0 & int & 0 & 1 & 0 & \partial_x & 0 \end{pmatrix}}_{\mathcal{J}} \underbrace{\begin{pmatrix} e_1 \\ e_{r1} \\ e_2 \\ e_{r2} \\ e_3 \\ e_4 \\ e_5 \\ e_6 \end{pmatrix}}_{e} + A_1\lambda_{\mathbf{L}}, \tag{28}$$

where $int = \int_Z B_a(\cdot)dz$, $A_1 = (0\ 0\ -(\partial_z \mathbf{1}_Z)\ 0\ 0\ 0\ 0\ B_p)^T$, with

$$A_1^* e = e_2\left(\frac{h}{2}\right) - e_2\left(-\frac{h}{2}\right) - B_p e_6 = 0. \tag{29}$$

Note that the operator $\partial_z \mathbf{1}_Z$ equals to zeros when multiplied by a variable outside the z domain (e.g. $\lambda_{\mathbf{L}}$), while equals to the difference at the boundary when multiplied by a variable belongs to its domain (e.g. $\partial_z \mathbf{1}_Z e_2 = -e_2(h/2) + e_2(-h/2)$).

Suppose the parameters C_2, K, A, ρ, E, and I are homogeneous, the Hamiltonian of this system is:

$$H(t) = \frac{1}{2}\int_x\int_\xi \frac{Q^2}{C_2}d\xi dx + \frac{1}{2}\int_x\int_z f_s^2 dz dx + \frac{1}{2}\int_x \left(GAx_3(x)^2 + \frac{x_4(x)^2}{\rho A} + EIx_5(x)^2 + \frac{x_6(x)^2}{\rho I}\right)dx. \tag{30}$$

3. DISCRETIZATION AND MODEL REDUCTION

In order to preserve the geometric structure of the overall PHS, the finite difference method on staggered grids (Trenchant et al., 2018) is employed to discretize each scale of the distributed parameter model of the system. The principle of this method is to approximate effort and flow variables on different grids in order to preserve the power balances. A particular care has to be paid on the boundary conditions and to interconnexions between two different scales. In a second instance a projection is used in order to get rid of the Lagrangian multipliers.

3.1 Multiscale discretization

Considering the fact that we have a multi-scale model, ξ and z are local coordinates while x is the global coordinate, which leads to the assumption that for each point in x, there is one corresponding ξ and z. Hence, there will be $N_e\,(= N_\xi \times N_b)$ elements for the electrical system, $N_g\,(= N_z \times N_b)$ ones for the electro-stress diffusion system, and N_b elements for the mechanical system. For a sake of conciseness the discretization method is not detailed here. It yields the final dimensional model below:

$$\underbrace{\begin{pmatrix}\dot{x_{1d}}\\ \dot{x}_{2d}\\ \dot{x}_{3d}\\ \dot{x}_{4d}\\ \dot{x}_{5d}\\ \dot{x}_{6d}\end{pmatrix}}_{\dot{x_d}} = \underbrace{\begin{pmatrix} M_2D_1^T & P_1 & 0 & 0 & 0 & 0\\ P_3 & P_2 & 0 & 0 & 0 & D_{26}\\ 0 & 0 & 0 & -D_6^T & 0 & -D_{63}^T\\ 0 & 0 & D_6 & 0 & 0 & 0\\ 0 & 0 & 0 & 0 & 0 & -D_6^T\\ 0 & -D_{26}^T & D_{63} & 0 & D_6 & 0\end{pmatrix}}_{J_r}\underbrace{\begin{pmatrix}e_{1d}\\ e_{2d}\\ e_{3d}\\ e_{4d}\\ e_{5d}\\ e_{6d}\end{pmatrix}}_{e_d} + \underbrace{\begin{pmatrix}-M_2\\ M_1(D_1^TL_{r2}M_2 - \mathcal{I})\\ 0\\ 0\\ 0\\ 0\end{pmatrix}}_{B} V + \underbrace{\begin{pmatrix}0\\ g_{21}+g_{22}\\ 0\\ 0\\ 0\\ diag(B_p)\end{pmatrix}}_{g_c}\lambda_{\mathbf{L}d}, \tag{31}$$

and the constraint equation

$$g_c^T e_d = 0. \tag{32}$$

where $x_{1d} = \left(Q^{1,1}\ \cdots\ Q^{N_\xi,N_b}\right)^T$, $x_{2d} = \left(f_s^{1,1}\ \cdots\ f_s^{N_z,N_b}\right)^T$, $x_{3d} = \left(x_3^1\ \cdots\ x_3^{N_b}\right)^T$, $x_{4d} = \left(x_4^1\ \cdots\ x_4^{N_b}\right)^T$, $x_{5d} = \left(x_5^1\ \cdots\ x_5^{N_b}\right)^T$, $x_{6d} = \left(x_6^1\ \cdots\ x_6^{N_b}\right)^T$, $e_d = L_d x_d$, $L_d = blockdiag\,(1/C_2, 1, GA, 1/(\rho A), EI, 1/(\rho I))$ of proper dimension, $L_{r1} = diag(-1/R_1)$, $L_{r2} = diag(-R_2)$, $L_{r3} = diag(-D')$, $M1 = \frac{\lambda}{\sigma_e Lb}(g_{21}+g_{22})g^T L_{r1}$, $M2 = (\mathcal{I} + D_1L_{r1}D_1^TL_{r2})^{-1}D_1L_{r1}$, $P_1 = \frac{\lambda}{\sigma_e Lb}M_2 g_2^T$, $P_2 = D_2^TL_{r3}D_2 - \frac{\lambda}{\sigma_e Lb}M_1(D_1^TL_{r2}M_2 + \mathcal{I})g(g_{21}+g_{22})^T$, $P_3 = M_1D_1^T(\mathcal{I} - L_{r2}M_2D_1^T)$. D_i with $i \in \{1, 26, 6, 63\}$ and g_k with $k \in \{21, 22\}$ are matrices depending on the discretization steps and systems parameters.

3.2 Elimination of Lagrangian multipliers

In this section the DAE (31) together with (32) will be reduced to an ODE, in order to perform the simulation and apply control strategies afterwards. The proposed method is based on the idea of coordinate projection as in (Wu et al., 2014). Given

$$M = \begin{pmatrix} S \\ (g_c^Tg_c)^{-1}g_c^T\end{pmatrix},$$

where S satisfies: $S \cdot g_c = 0$.

Now define $X_1 = (x_{1d}\ x_{2d}\ x_{3d}\ x_{4d}\ x_{5d})^T$, $X_2 = x_{6d}$, $\left(\tilde{X}_1\ \tilde{X}_2\right)^T = M\,(X_1\ X_2)^T$,

$B_1 = \left(-M_2^T\ \left(M_1(D_1^TL_{r2}M_2 - \mathcal{I})\right)^T\ 0\ 0\ 0\right)^T$ and $B_2 = 0$. Equation (31) is multiplied by the matrix M, and becomes:

$$\begin{pmatrix}\dot{\tilde{X}}_1\\ \dot{\tilde{X}}_2\end{pmatrix} = \underbrace{MJ_rM^T}_{\tilde{J}_r}\underbrace{M^{-T}L_dM^{-1}}_{\tilde{L}_d}\begin{pmatrix}\tilde{X}_1\\ \tilde{X}_2\end{pmatrix} + \begin{pmatrix}MB_1\\ 0\end{pmatrix}V + \begin{pmatrix}0\\ I\end{pmatrix}\lambda_{\mathbf{L}d} \tag{33}$$

Meanwhile, equation (32) can be rewritten as:

$$\underbrace{g_c^TM^T}_{\tilde{g}_c}\tilde{L}_d\begin{pmatrix}\tilde{X}_1\\ \tilde{X}_2\end{pmatrix} = 0 \tag{34}$$

It is implied from equation (33) that $\tilde{X}_1$ does not depend on $\lambda_{\mathbf{L}d}$. Hence the second line of equation (33) is substituted by equation (34), reforming a descriptor system as follows:

$$\begin{pmatrix}I & 0\\ 0 & 0\end{pmatrix}\begin{pmatrix}\dot{\tilde{X}}_1\\ \dot{\tilde{X}}_2\end{pmatrix} = \begin{pmatrix}\tilde{J}_{11} & \tilde{J}_{12}\\ \tilde{g}_c\end{pmatrix}\begin{pmatrix}\tilde{L}_{d11} & \tilde{L}_{d12}\\ \tilde{L}_{d21} & \tilde{L}_{d22}\end{pmatrix}\begin{pmatrix}\tilde{X}_1\\ \tilde{X}_2\end{pmatrix} + \begin{pmatrix}MB_1\\ 0\end{pmatrix}V \tag{35}$$

4. SIMULATION

In this section, the proposed model will be verified by comparing the simulation with the experimental results. The simulation carries out with an IPMC actuator of dimension $45mm$ (in length)$\times 5mm$ (in width)$\times 0.2mm$ (in height), which contains the tetraethyl-ammonium ion TEA^+, and whose total resistance and capacitance equal to $23.6178\,\Omega$ and $0.0635\,F$, respectively. Mechanical parameters of this IPMC are illustrated in table 1. With a voltage $1V$ applied, the deformation of the endpoint of the IPMC strip and the output current are shown in Fig. 6. From Fig. 6, one can observe the simulation reproduces the same behaviors of the experimental results.

5. CONCLUSION

In this article, a detailed IPMC model is characterized under the port-Hamiltonian framework, and its dynamic

Table 1. Parameters values

Par.	Value	Unit	Par.	Value	Unit
ρ [1]	1.633×10^3	kg/m^3	λ	16.6×10^{-9}	$m^2/(Vs)$
E [2]	9×10^7	Pa	σ_e	3.274×10^{-3}	$1/(\Omega m)$
v [3]	0.3	1	D'	1.375×10^{-11}	m^2/s
k	8.53×10^{-14}	$m^3 s/kg$			

[1] Material density.
[2] Young's modulus.
[3] Poisson ratio.

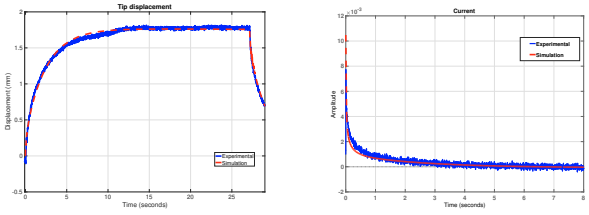

Fig. 6. Displacement of the endpoint of the IPMC and current.

performance is investigated numerically. The Lagrangian multiplier method is used to model the geometric constraints between the gel and the beam. The global system forms a stokes-Dirac structure, that guarantees the energy preservation. This system is later discretized by means of the finite difference method on staggered grids. Thus, the model can be reduced into a descriptor port-Hamiltonian form with the elimination of the Lagrangian multiplier. Finally, the proposed model has been validated by the experimental measurements. The ongoing work is to deal with the modeling of the 2-D tubular IPMC actuator. Also, the passivity based control design for the IPMC actuator would be investigated under the port-Hamiltonian framework in the future.

REFERENCES

Bao, X., Bar-Cohen, Y., and Lih, S.S. (2002). Measurements and macro models of ionomeric polymer-metal composites (ipmc). In *Smart Structures and Materials 2002: Electroactive Polymer Actuators and Devices (EAPAD)*, volume 4695, 220–228. International Society for Optics and Photonics.

Branco, P.C., Lopes, B., and Dente, J. (2012). Nonuniformly charged ionic polymer–metal composite actuators: Electromechanical modeling and experimental validation. *IEEE Trans. on Ind. Elec.*, 59(2), 1105–1113.

De Gennes, P., Okumura, K., Shahinpoor, M., and Kim, K.J. (2000). Mechanoelectric effects in ionic gels. *EPL (Europhysics Letters)*, 50(4), 513.

Le Gorrec, Y., Zwart, H., and Maschke, B. (2005). Dirac structures and boundary control systems associated with skew-symmetric differential operators. *SIAM journal on control and optimization*, 44(5), 1864–1892.

Maschke, B. and van der Schaft, A. (1992). Port-controlled hamiltonian systems: Modelling origins and systemtheoretic properties. *IFAC Proceedings Volumes*, 25(13), 359 – 365. 2nd IFAC Symposium on Nonlinear Control Systems Design 1992, Bordeaux, France, 24-26 June.

Nishida, G., Takagi, K., Maschke, B., and Luo, Z.w. (2008). Multi-scale distributed port-hamiltonian representation of ionic polymer-metal composite. In *Proceedings of the 17th IFAC World Congress*, volume 17.

Nishida, G., Takagi, K., Maschke, B., and Osada, T. (2011). Multi-scale distributed parameter modeling of ionic polymer-metal composite soft actuator. *Control Engineering Practice*, 19(4), 321–334.

Park, K., Yoon, M.K., Lee, S., Choi, J., and Thubrikar, M. (2010). Effects of electrode degradation and solvent evaporation on the performance of ionic-polymer–metal composite sensors. *Smart Materials and Structures*, 19(7), 075002.

Shahinpoor, M. (ed.) (2016). *Ionic Polymer Metal Composites (IPMCs)*, volume 1 of *Smart Materials Series*. The Royal Society of Chemistry. doi: 10.1039/9781782622581.

Trenchant, V., Ramirez, H., Le Gorrec, Y., and Kotyczka, P. (2018). Finite differences on staggered grids preserving the port-hamiltonian structure with application to an acoustic duct. *Journal of Computational Physics*, 373, 673–697.

Villegas, J.A. (2007). A port-hamiltonian approach to distributed parameter systems.

Wu, Y., Hamroun, B., Le Gorrec, Y., and Maschke, B. (2014). Port hamiltonian system in descriptor form for balanced reduction: Application to a nanotweezer. *IFAC Proceedings Volumes*, 47(3), 11404–11409.

Xiao, Y. and Bhattacharya, K. (2001). Modeling electromechanical properties of ionic polymers. In *Smart Structures and Materials 2001: Electroactive Polymer Actuators and Devices*, volume 4329, 292–301. International Society for Optics and Photonics.

Yamaue, T., Mukai, H., Asaka, K., and Doi, M. (2005). Electrostress diffusion coupling model for polyelectrolyte gels. *Macromolecules*, 38(4), 1349–1356.

Zhu, Z., Chen, H., Wang, Y., and Li, B. (2012). Multiphysical modeling for electro-transport and deformation of ionic polymer metal composites. In *Electroactive Polymer Actuators and Devices (EAPAD)*, volume 8340. Int. Soc. for Optics and Photonics.